Supplementary Information (SREP-12-03460)

Controlled Assembly of Sb_2S_3 Nanoparticles on Silica/Polymer Nanotubes: Insights into the Nature of Hybrid Interfaces

Huaming Yang, Mei Li, Liangjie Fu, Aidong Tang & Stephen Mann

Table S1 Comparison of lattice parameters for various samples

Sample	*a* (Å)	*b* (Å)	*c* (Å)	Lattice volume (Å^3)
calcined Sb_2S_3	11.226	11.321	3.838	487.81
calcined Sb_2S_3/HNTs	11.226	11.307	3.835	486.82
Sb_2S_3 (JCPDS 06-0474)	11.229	11.310	3.839	487.55

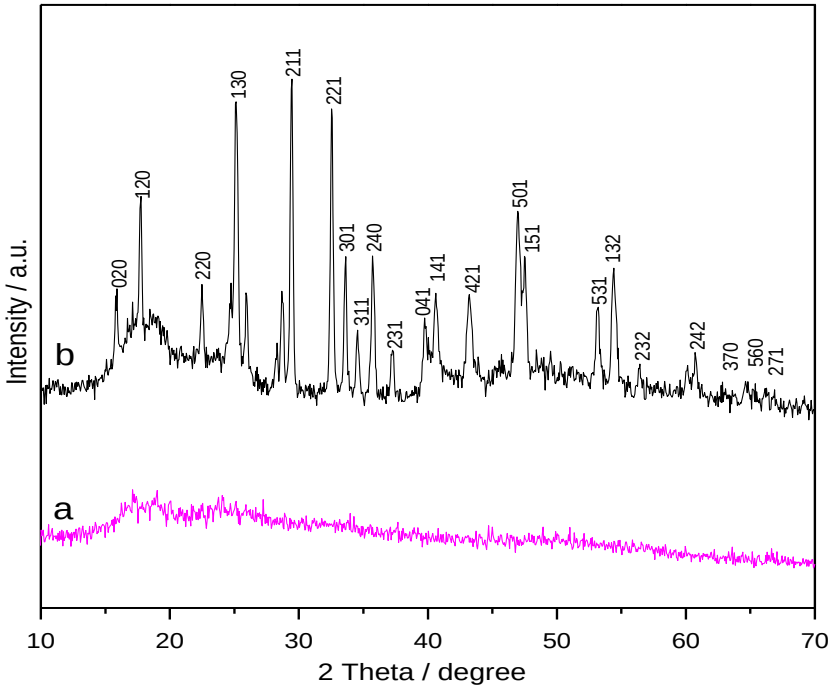

Figure S1 XRD patterns of (a) as-synthesized Sb_2S_3 and (b) calcined Sb_2S_3 at 400 ºC under N_2.

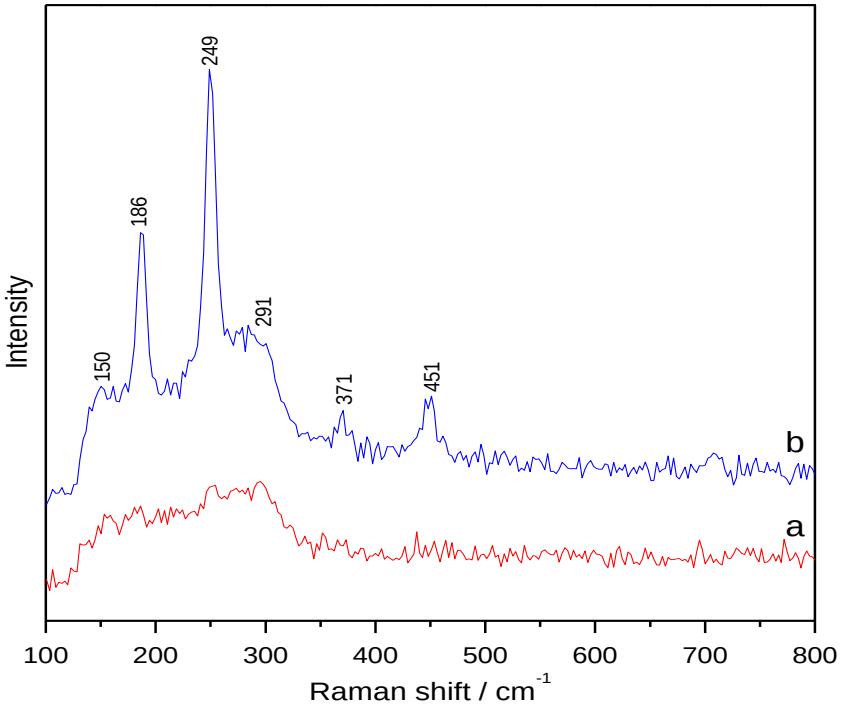

Figure S2 Raman spectra of (a) as-synthesized Sb_2S_3/HNTs and (b) heated Sb_2S_3/HNTs at 400 ºC under N_2.

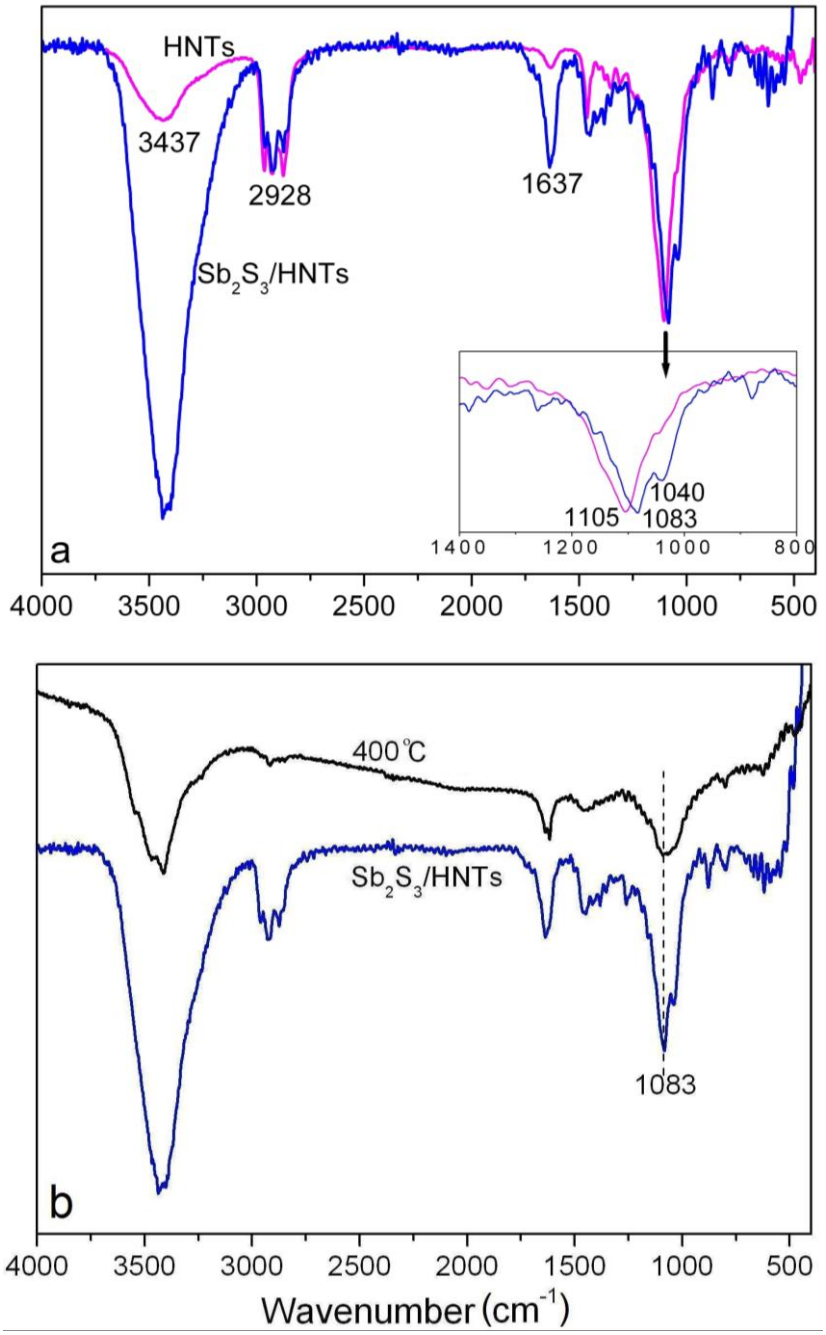

Figure S3 (a) FTIR spectra of HNTs and as-synthesized Sb_2S_3/HNTs. The large increase in the intensity of the O–H and $–NH_s$ stretching vibrations at 3437 cm^{-1}, and C=O stretching vibration at 1637 cm^{-1}, as well as the appearance of a C-N stretching vibration at 1040 cm^{-1}, is associated with the acetamide byproduct of the reaction of TAA with antimony chloride. (b) FTIR spectra of as-synthesized Sb_2S_3/HNTs and calcined Sb_2S_3/HNTs at 400 ºC under N_2.

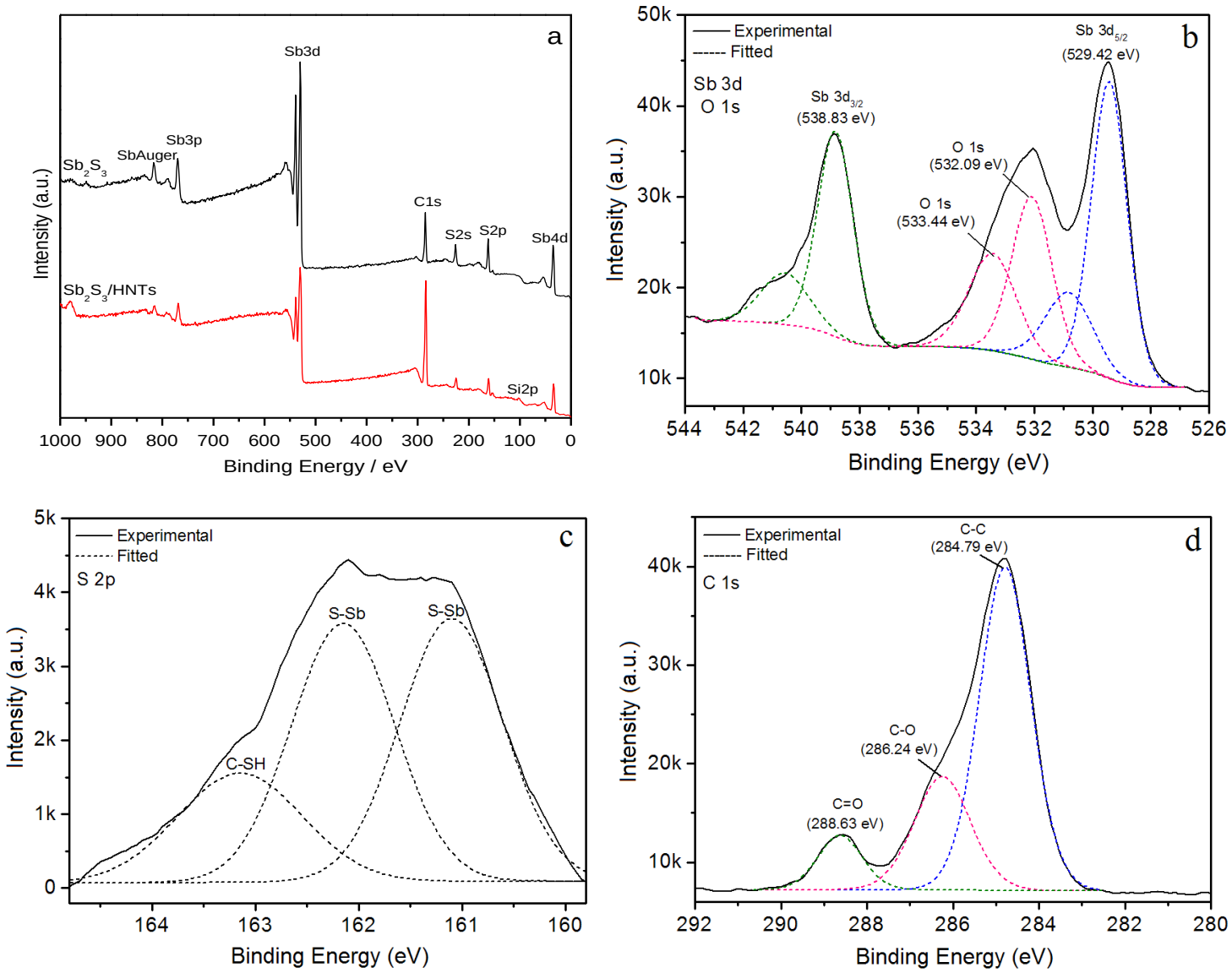

Figure S4 (a) XPS survey spectra of the as-synthesized Sb_2S_3 and Sb_2S_3/HNTs**.** Trace amounts of carbon in the control sample originate from residual impurities during the synthesis procedure. High-resolution XPS profiles and fitted lines for (b) Sb 3d and O 1s, (c) S 2p and (d) C 1s regions for as-synthesized Sb_2S_3/HNTs.

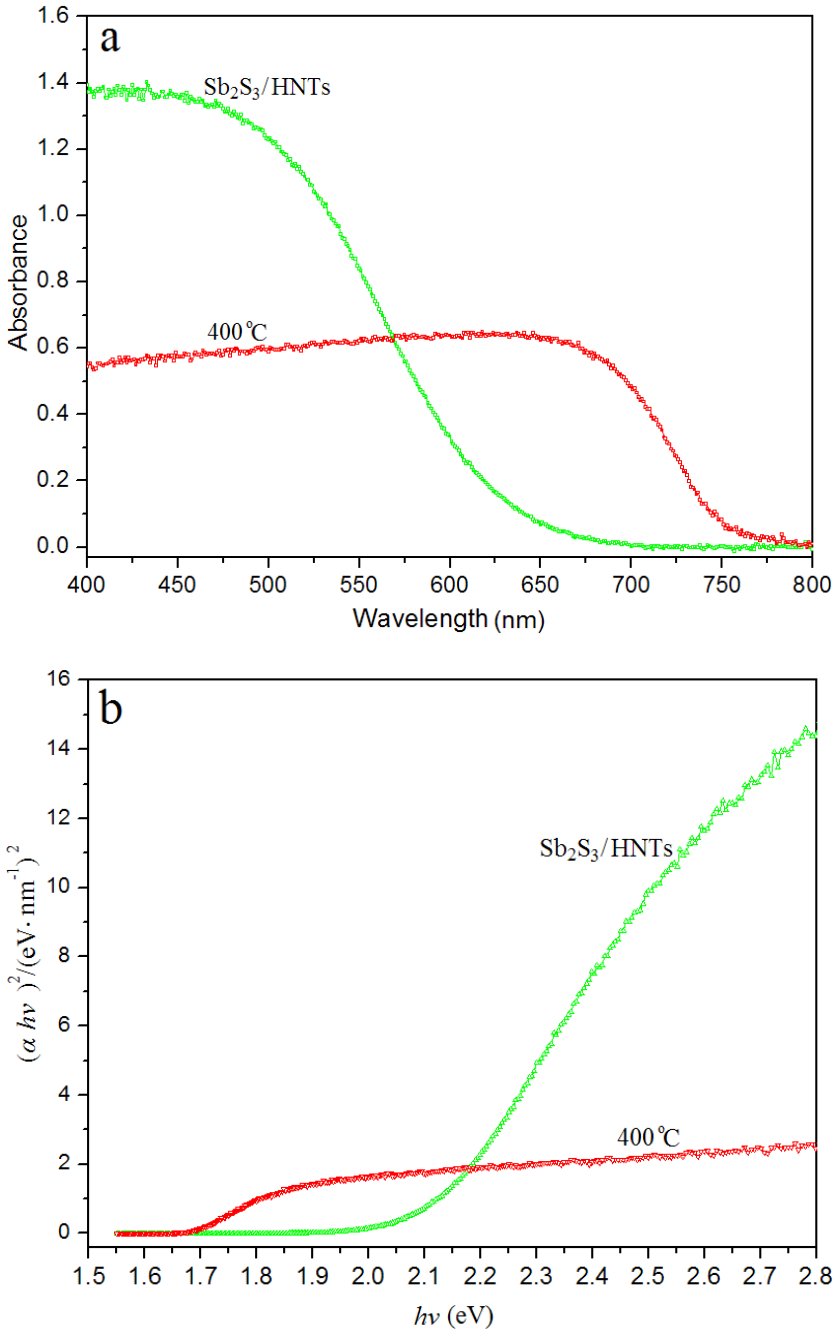

Figure S5 (a) Solid-state UV-vis spectra and (b) plots of $(\alpha hv)^2$ versus hv of as-synthesized Sb_2S_3/HNTs and the calcined Sb_2S_3/HNTs at 400 ºC under N_2.

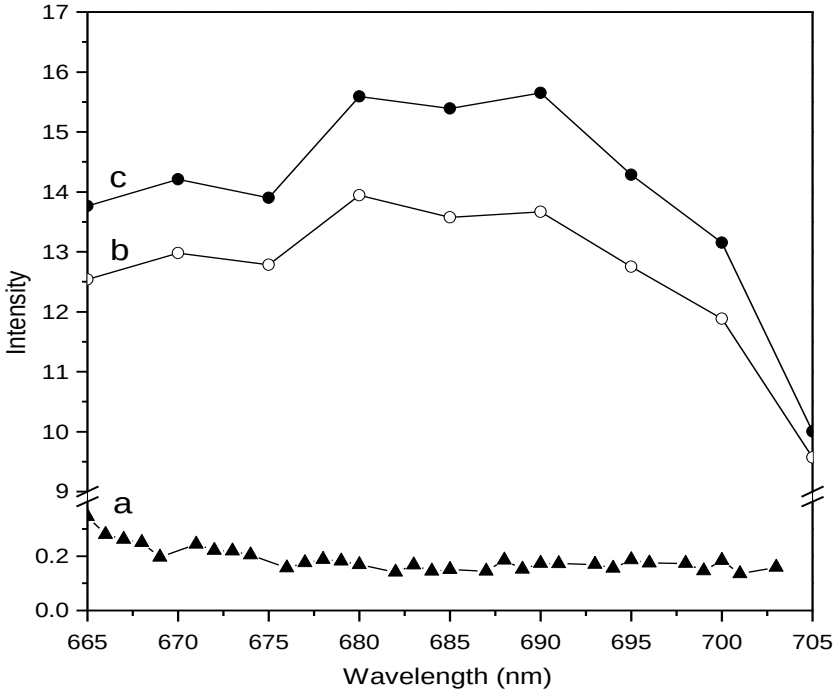

Figure S6 Fluorescence spectra of (a) original HNTs, (b) as-synthesized Sb_2S_3 and (c) Sb_2S_3/HNTs.

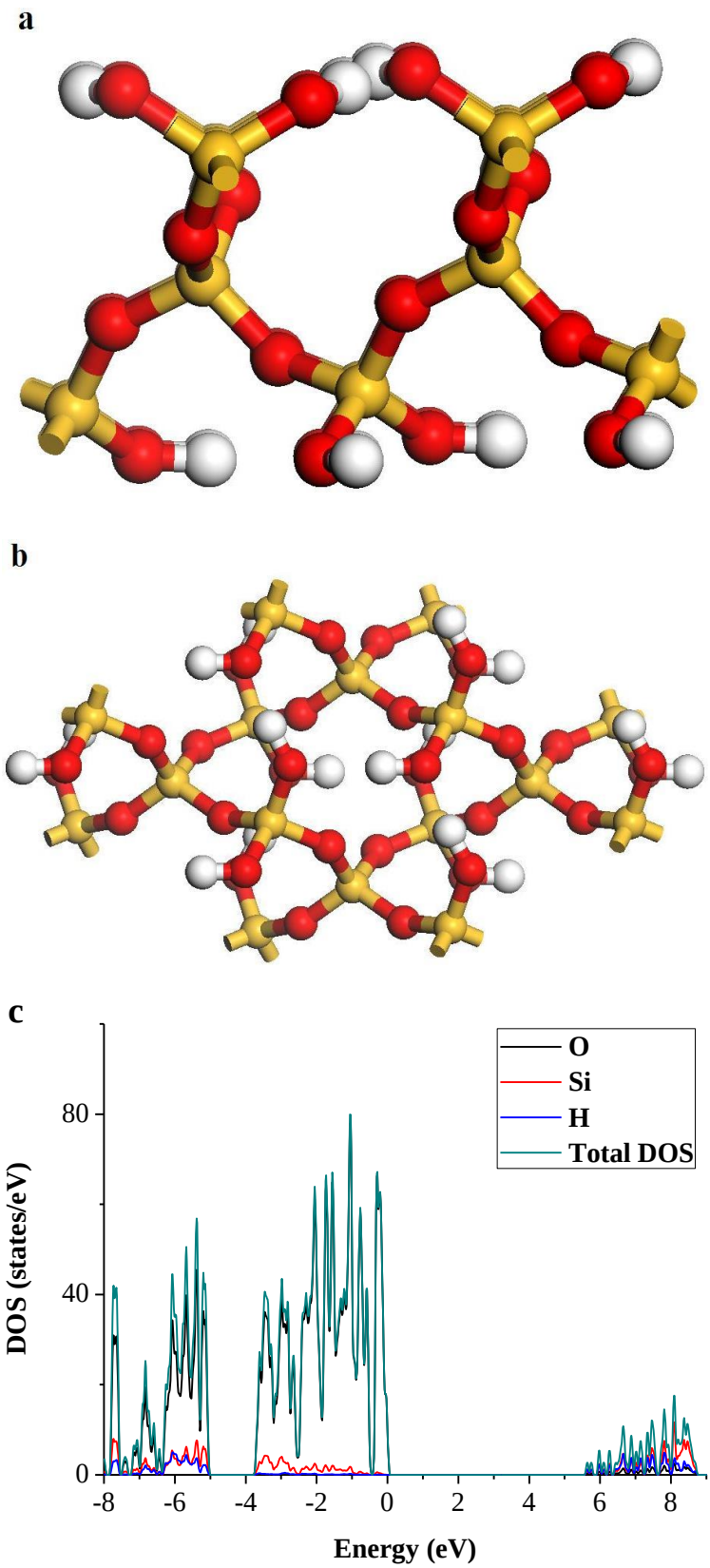

Figure S7 Structural model of amorphous silica surface. (a) Side view, (b) top view, and (c) corresponding total density of states (DOS) and atom-projected density of states (PDOS).

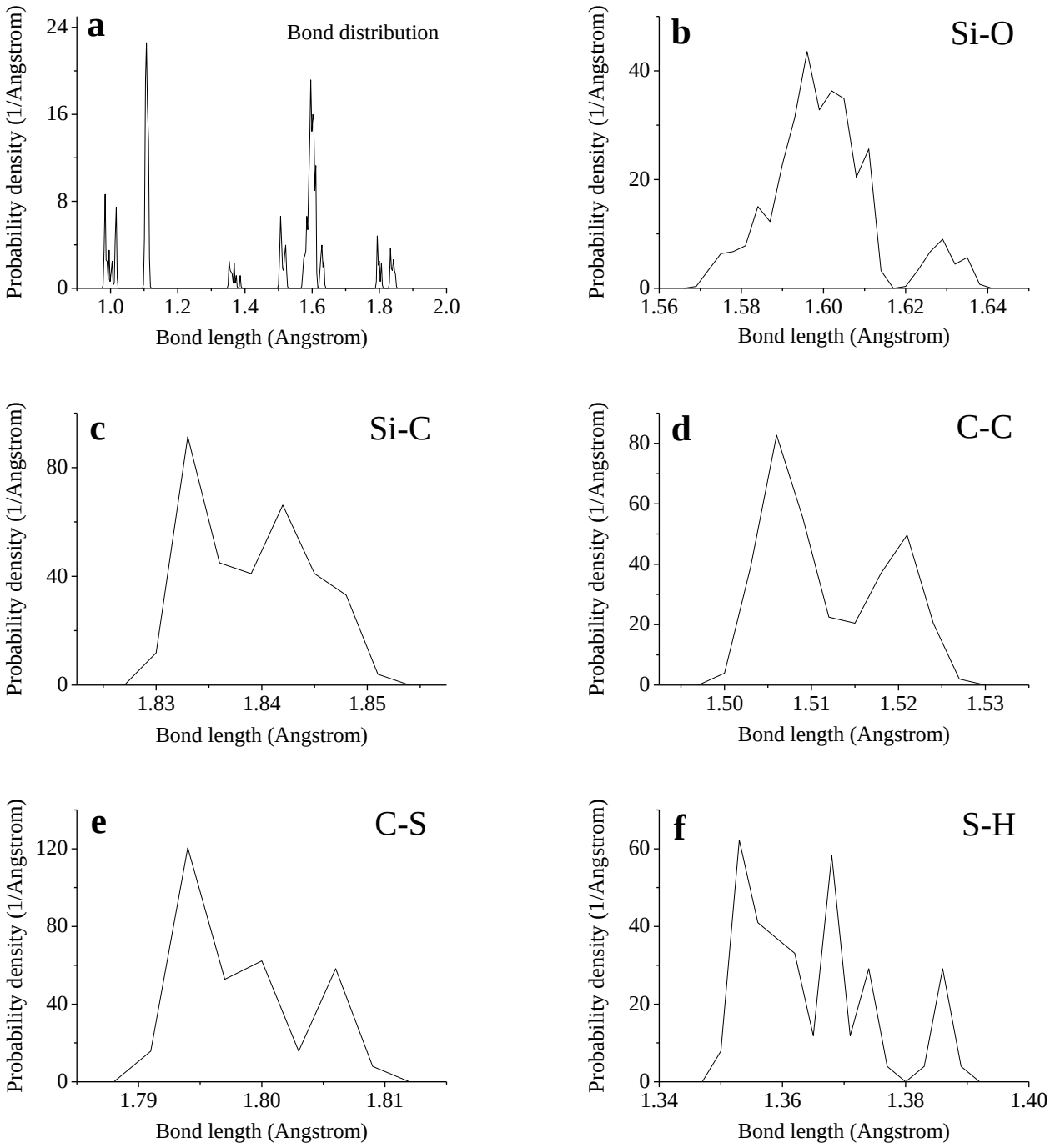

Figure S8 Bond length distributions of the HNTs surface.

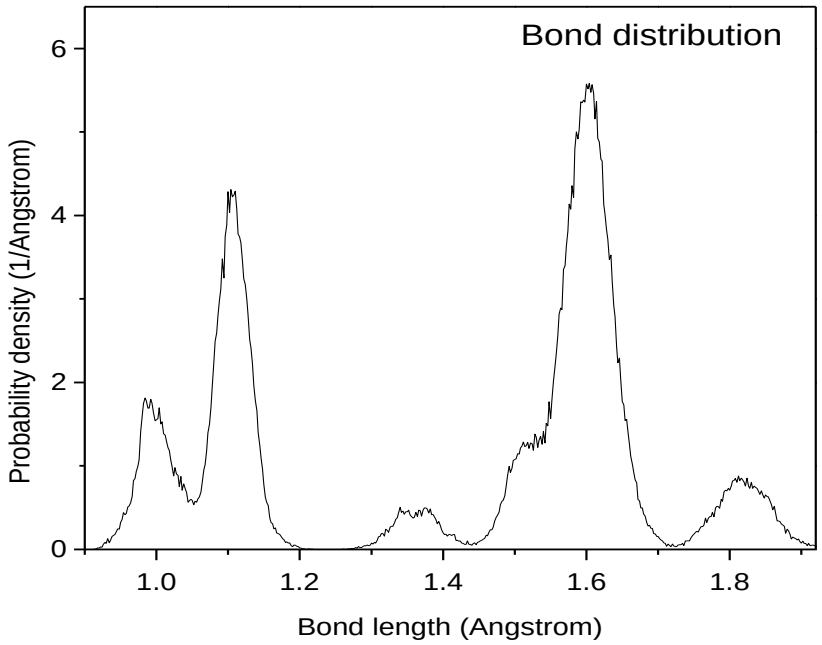

Figure S9 Bond length distribution on a mercaptopropyl-functionalized amorphous silica surface after 5 ps dynamic equilibrium.

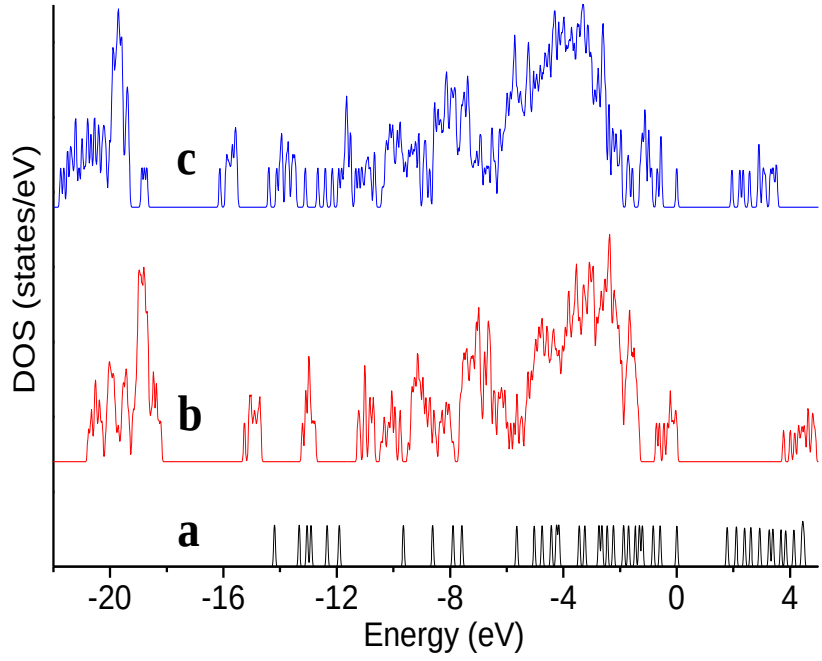

Figure S10 Total density of states (DOS). The calculated band gaps were: (a) pure Sb_2S_3 (1.75 eV), (b) mercaptopropyl-functionalized silica surface (HNTs, 3.75 eV), and (c) Sb_2S_3/HNT nanocomposites (2.0 eV). The latter two values agreed well with the experimental results (solid-state UV-vis spectroscopy, Figure S5). The underestimate of the band gap is mainly due to the well-known LDA problem, but it does not influence the theoretical analysis.

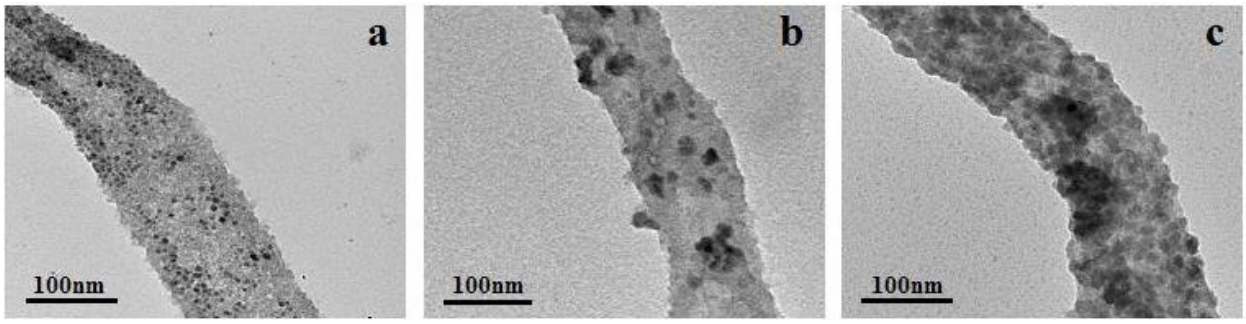

Figure S11 TEM images of the individual HNT coated with Sb_2S_3 nanoparticles for the as-synthesized Sb_2S_3/HNTs prepared by simultaneously adding TAA and HNTs to a Sb(III) solution at Sb:Si molar ratio of (a) 1:1 and (b) 1:10. (c) Sample prepared by adding TAA followed by a HNTs suspension.

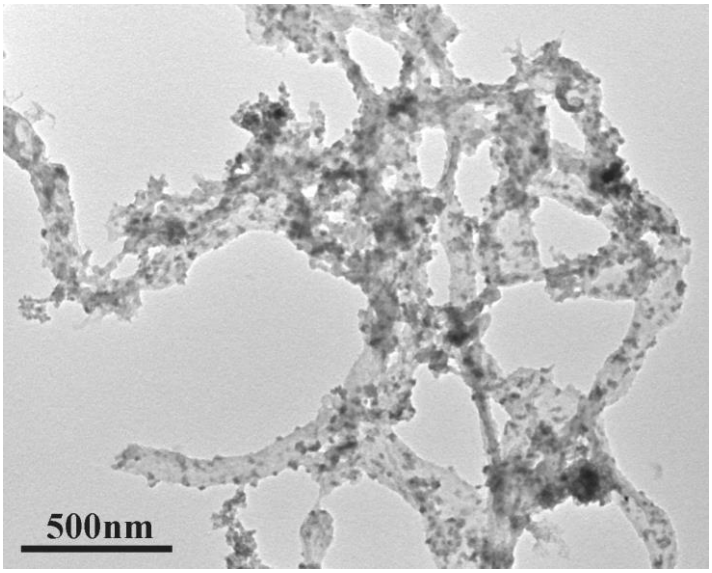

Figure S12 Low magnification TEM image of as-synthesized Sb_2S_3/HNTs at Sb:Si=1:10.